



УДК 536.625:539.25:539.651

DOI 10.17073/0368-0797-2023-6-666-672



Оригинальная статья

Original article

## ANALYSIS OF CONTACT ZONE OF COATING-SUBSTRATE SYSTEM EXPOSED TO IRRADIATION WITH A PULSE ELECTRON BEAM

M. O. Efimov<sup>1</sup>, Yu. F. Ivanov<sup>2</sup>, V. E. Gromov<sup>1</sup>Yu. A. Shlyarova<sup>1</sup>, I. A. Panchenko<sup>1</sup><sup>1</sup> Siberian State Industrial University (42 Kirova Str., Novokuznetsk, Kemerovo Region – Kuzbass 654007, Russian Federation)<sup>2</sup> Institute of High Current Electronics, Siberian Branch of the Russian Academy of Sciences (2/3 Academiceskii Ave., Tomsk 634055, Russian Federation)

gromov@physics.sibsiu.ru

**Abstract.** Using the wire-arc additive manufacturing method (WAAM) on a 5083 aluminum alloy substrate, a non-equiautomic Mn–Cr–Fe–Co–Ni high-entropy alloy (HEA) coating was formed. By scanning and transmission electron diffraction microscopy we analyzed the structure, phase and elemental composition of the contact zone after irradiation with high-current low-energy electron beams with the following parameters: accelerated electron energy 18 keV, electron beam energy density 30 J/cm<sup>2</sup>, electron beam pulse duration 200 μs, number of pulses 3, pulse repetition rate 0.3 s<sup>-1</sup>. Multiphase multielement submicro- and nanocrystalline structures are formed predominantly in the substrate, which has a lower melting temperature compared to HEAs. Mutual doping of the coating – substrate system occurs in the contact layer, which has sinuous boundaries. The contact layers adjacent to the substrate and coating have the structure of high-speed cellular crystallization. In the layer adjacent to the substrate, the cells are formed by a solid solution of magnesium in aluminum. Interlayers of the second phase, enriched in atoms of the coating and substrate, are revealed along the cell boundaries. In the layer adjacent to the coating, the cells are formed by an alloy of composition 0.17Mg – 20.3Al – 4.3Cr – 16.7Fe – 9.3Co – 49.2Ni corresponding to the coating. Interlayers of the second phase, enriched mainly in magnesium and, to a lesser extent, in atoms of the HEA coating, are located along the cell boundaries. Central region of the contact zone with a thickness of ~1700 μm is formed by lamellar crystallites, which indicates the eutectic nature of its formation. Its main element is aluminum (~77 at. %).

**Keywords:** high-entropy alloy, 5083 alloy, wire-arc additive manufacturing method, pulsed electron beam, elemental and phase composition, structure, contact zone

**Acknowledgements:** The work was supported by the Russian Science Foundation, project no. 20-19-00452 and grant no. 19-19-00183, <https://rscf.ru/project/19-19-00183/>.

**For citation:** Efimov M.O., Ivanov Yu.F., Gromov V.E., Shlyarova Yu.A., Panchenko I.A. Analysis of contact zone of coating-substrate system exposed to irradiation with a pulse electron beam. *Izvestiya. Ferrous Metallurgy.* 2023;66(6):666–672.

<https://doi.org/10.17073/0368-0797-2023-6-666-672>

## АНАЛИЗ ЗОНЫ КОНТАКТА СИСТЕМЫ ПОКРЫТИЕ – ПОДЛОЖКА, ПОДВЕРГНУТОЙ ОБЛУЧЕНИЮ ИМПУЛЬСНЫМ ЭЛЕКТРОННЫМ ПУЧКОМ

M. O. Ефимов<sup>1</sup>, Ю. Ф. Иванов<sup>2</sup>, В. Е. Громов<sup>1</sup>Ю. А. Шлярова<sup>1</sup>, И. А. Панченко<sup>1</sup><sup>1</sup> Сибирский государственный индустриальный университет (Россия, 654007, Кемеровская обл. – Кузбасс, Новокузнецк, ул. Кирова, 42)<sup>2</sup> Институт сильноточной электроники Сибирского отделения РАН (Россия, 634055, Томск, пр. Академический, 2/3)

gromov@physics.sibsiu.ru

**Аннотация.** Методом проволочно-дугового аддитивного производства (WAAM – *wire arc additive manufacturing*) на подложке из алюминиевого сплава 5083 сформировано покрытие из высоконентропийного сплава Mn–Cr–Fe–Co–Ni неэквивалентного состава. Методами сканирующей и просвечивающей электронной дифракционной микроскопии выполнен анализ структуры, фазового и элементного состава зоны контакта после облучения сильноточными низкоэнергетическими электронными пучками с параметрами: энергия ускоренных электронов 18 кэВ; плотность энергии пучка электронов 30 Дж/см<sup>2</sup>; длительность импульса пучка электронов 200 мкс; количество импульсов 3; частота следования импульсов 0,3 с<sup>-1</sup>. Многофазная многоэлементная субмикро- и нанокристал-

лическая структуры формируются преимущественно в подложке, которая имеет более низкую температуру плавления по сравнению с ВЭС. В контактном слое, имеющем извилистые границы, происходит взаимное легирование системы покрытие – подложка. Контактные слои, примыкающие к подложке и покрытию, имеют структуру высокоскоростной ячеистой кристаллизации. В слое, примыкающем к подложке, ячейки образованы твердым раствором магния в алюминии. По границам ячеек находятся прослойки второй фазы, обогащенные атомами покрытия и подложки. В слое, примыкающем к покрытию, ячейки сформированы сплавом состава 0,17 % Mg – 20,3 % Al – 4,3 % Cr – 16,7 % Fe – 9,3 % Co – 49,2 % Ni, соответствующего покрытию. По границам ячеек располагаются прослойки второй фазы, обогащенные преимущественно магнием и в меньшей степени атомами покрытия ВЭС. Центральная область зоны контакта толщиной примерно 1700 мкм сформирована кристаллитами пластинчатой формы, что свидетельствует об эвтектической природе ее образования. Ее основным элементом является алюминий (примерно 77 % (ат.)).

**Ключевые слова:** высоконтропийный сплав, сплав 5083, метод проволочно-дугового аддитивного производства, импульсный электронный пучок, элементный и фазовый состав, структура, зона контакта

**Благодарности:** Работа выполнена при финансовой поддержке Российского научного фонда, грант № 20-19-00452 и грант № 19-19-00183, <https://rscf.ru/project/19-19-00183/>.

**Для цитирования:** Ефимов М.О., Иванов Ю.Ф., Громов В.Е., Шлярова Ю.А., Панченко И.А. Анализ зоны контакта системы покрытие – подложка, подвергнутой облучению импульсным электронным пучком. *Известия вузов. Черная металлургия*. 2023;66(6):666–672.

<https://doi.org/10.17073/0368-0797-2023-6-666-672>

## INTRODUCTION

Over the past two decades, there has been a notable surge in scientific interest regarding the development and investigation of high-entropy alloys (HEAs) owing to their distinctive microstructure, composite composition, and exceptional mechanical and functional properties [1; 2]. The pioneering materials in this category were alloys within the Al–Co–Cr–Fe–Ni systems and the Cantor alloy Mn–Co–Cr–Fe–Ni [3; 4]. HEAs, beyond possessing characteristics typical of conventional metal alloys, exhibit unique and unconventional properties reminiscent of metal-ceramics. These include high hardness and resistance to temperature hardening, dispersion hardening, a positive temperature hardening coefficient, elevated temperature strength, high wear and corrosion resistance, among other attributes [5 – 8].

Various reviews [8 – 11] have comprehensively analyzed the structural-phase states, properties, simulation, production methods, and application areas of the most promising HEAs. It has been emphasized that the advent of HEAs represents a significant leap forward in the advancement of metal alloys.

Currently, there is a wealth of information being actively accumulated on high-entropy alloys (HEAs), encompassing structural-phase states, defect substructure, stability, deformation behavior over a broad temperature range, the impact of doping and other factors, as well as novel methods for HEA production [12 – 17]. In the realm of HEA physics, there is a distinct focus on enhancing surface properties through various treatments, including irradiation with low-energy high-current electron beams. Electron-beam processing offers ultrahigh surface heating rates (up to  $10^8$  K/s) and subsequent cooling through heat-water transfer to the material's bulk. This leads to the formation of nonequilibrium submicro- and nanocrystalline structural-phase states, the development of a columnar structure, and the homogenization of chemical composition [18].

The primary objective of the current study is to analyze the structural-phase states within the contact zone of the HEA layer (coating) formed by wire-arc additive manufacturing on alloy 5083 (substrate) and subjected to electron-beam treatment.

## MATERIALS AND METHODS

The material under investigation in this study comprised a coating – substrate system. The coating was a high-entropy alloy with the elemental composition Mn–Cr–Fe–Co–Ni, fabricated onto the substrate using wire-arc additive manufacturing [1; 2]. The substrate material employed was alloy 5083. The contact zone of the coating–substrate system underwent irradiation with an intense pulsed electron beam using the SOLO installation. The process parameters for the irradiation were as follows: accelerated electrons' energy  $U = 18$  keV, electron beam energy density  $E_S = 30$  J/cm<sup>2</sup>, electron beam pulse duration  $t = 200$  μs, number of pulses  $N = 3$ , and pulse repetition rate  $f = 0.3$  s<sup>-1</sup>. The irradiation took place in a vacuum at a residual gas pressure (argon) in the installation chamber of  $p = 0.02$  Pa. To investigate the structural phase states of the contact zone between the coating and the substrate, scanning electron microscopy (SEM 515 Philips with EDAX ECON IV X-ray spectral microanalyzer) and transmission diffraction electron microscopy (JEM-2100) were employed [19 – 21]. Foils for the transmission electron microscope were prepared through ion thinning (Ion Slicer EM-091001S, utilizing argon ions) of plates obtained from bulk samples using an Isomet Low Speed Saw unit. The cutting was performed perpendicular to the surface of the HEA deposited layer, extending from the interface between the substrate and the deposit. This method facilitated the observation of structural and phase composition changes in the material with distance from the contact zone of the coating with the substrate.

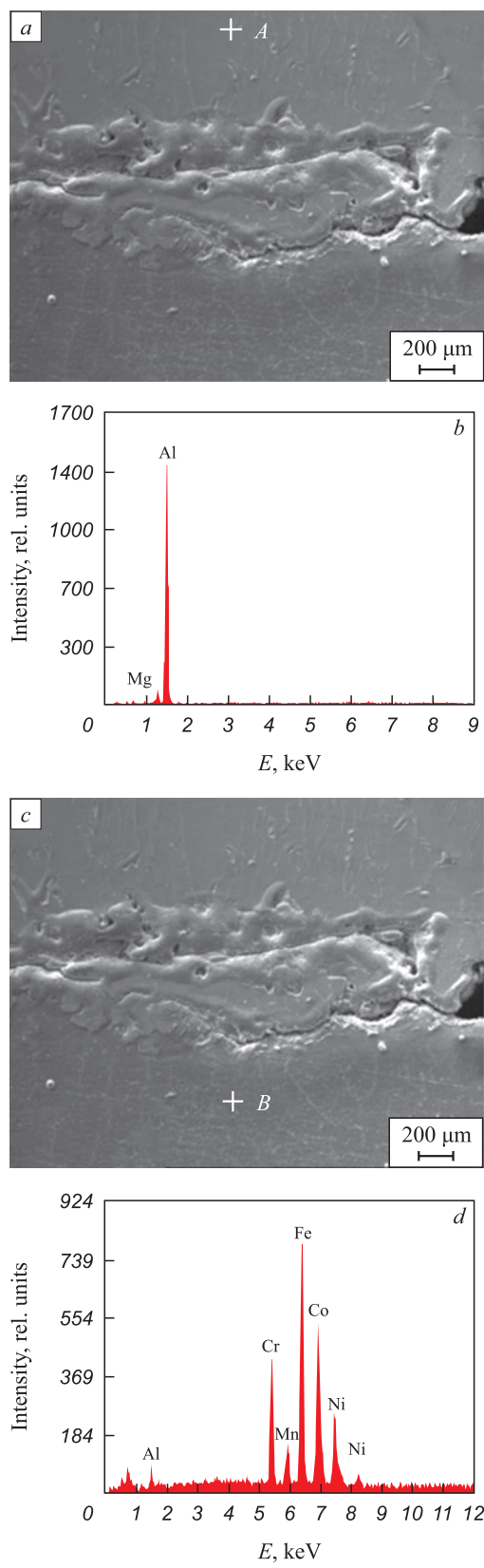


Fig. 1. Structure of the contact zone of HEA surfacing and substrate (AMg5) irradiated with a pulsed electron beam (a, c) and energy spectra obtained from regions A (b) and B (d)

Рис. 1. Структура области контакта наплавки ВЭС и подложки (AMg5), облученной импульсным электронным пучком (a, c) и энергетические спектры, полученные с области A (b) и области B (d)

## RESULTS AND DISCUSSION

In Fig. 1, an electron microscopic image displays the cross-section of the contact zone between the coating (HEA) and the substrate (alloy 5083). An extended layer, up to 700 μm thick, is evident, characterized by microcracks along the contact boundary on the substrate side. The sinuous boundaries of the contact layer suggest a high degree of fusion between the substrate and deposited material.

X-ray spectral microanalysis revealed mutual diffusion of atoms from the substrate and coating, as indicated in Table 1. Notably, the near-contact layer of the coating shows aluminum doping (Fig. 1, a, b, analysis region A), while the near-contact layer of the substrate exhibits doping with HEA elements (Fig. 1, c, d, analysis region B). Significantly, aluminum is more pronounced as a dopant in the coating, likely attributed to its lower melting point compared to HEA. Fig. 2 illustrates the change in elemental composition in the contact layer of the film – substrate system during the transition from the surfacing metal to the substrate metal (Fig. 2, b). A smooth transition in the elemental composition of the contact zone suggests the absence of vortex flows in the employed method of coating deposition on the substrate and subsequent irradiation with a pulsed electron beam.

Under the conditions of irradiation with a pulsed electron beam, mutual doping of the coating and substrate is expected to result in a significant alteration of the phase composition in the contact zone. The elemental and phase compositions were investigated using thin foil methods in layers (Fig. 2, b).

The examination revealed that the structure of layer I is characterized by cells displaying high-speed crystallization (Fig. 3, a). As it moves away from the contact zone with the coating, the cellular structure transforms into a layered structure (Fig. 3, b). The majority of cells constitute a solid solution of magnesium in aluminum, consistent with alloy 5083 (Table 2, analysis regions 1 and 2 are indicated in Fig. 3). Second-phase layers

Table 1

### Results of microrentgenospectral analysis of elemental composition of the coating in A region and the substrate in B region

Таблица 1. Результаты микрорентгеноспектрального анализа элементного состава покрытия в области А и подложки в области Б

Region	Content, at. %						
	Mg	Al	Cr	Mn	Fe	Co	Ni
A	5.7	92.4	0.3	0.5	0.5	0.3	0.3
B	0	12.3	12.6	2.7	32.5	25.3	14.6

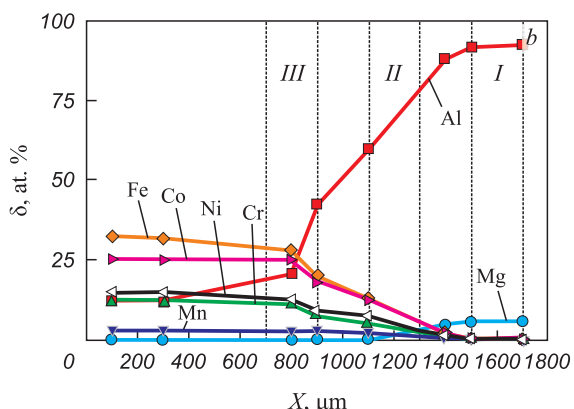
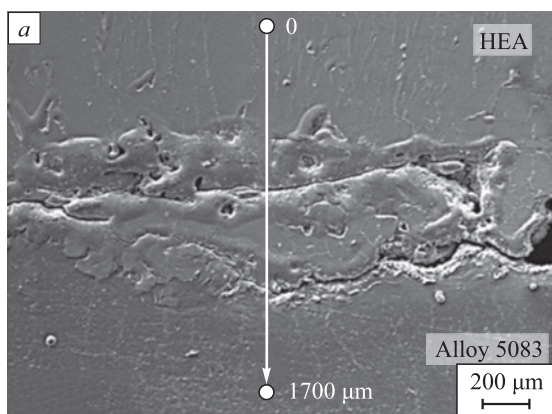


Fig. 2. Dependences of alloying elements concentration (*b*) of the contact zone of coating and substrate identified along the line (0 – 1700) shown on *a* (I, II, III – layers in which the analysis of structural-phase states was carried out by TEM and STEM methods)

Рис. 2. Зависимости концентрации легирующих элементов (*b*) зоны контакта покрытия и подложки, выявленные вдоль линии (0 – 1700), приведенной на поз. *a* (цифрами I, II, III обозначены слои, в которых осуществлялся анализ структурно-фазовых состояний методами TEM и STEM)

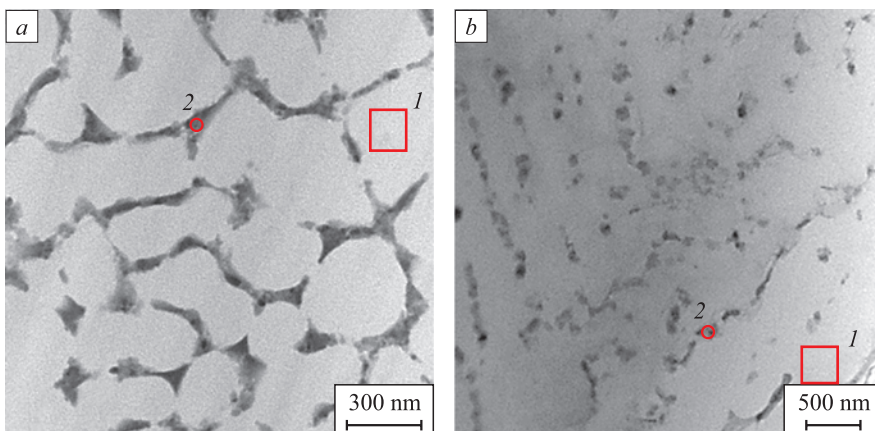


Fig. 3. Structure of layer *I* of the surfacing – substrate system irradiated by a pulsed electron beam (1 and 2 – areas of microrentgenospectral analysis of the alloy elemental composition)

Рис. 3. Структура слоя *I* системы «наплавка – подложка», облученной импульсным электронным пучком (цифрами 1 и 2 обозначены области микрорентгеноспектрального анализа элементного состава сплава)

at the cell boundaries are enriched with atoms from both the surfacing and substrate.

Through darkfield analysis with subsequent micro-electronogram identification, it was determined that the majority of high-speed crystallization cells were formed by a solid solution based on aluminum. These cells are separated by layers of the Mg<sub>2</sub>Si phase.

Layer *II* exhibits a lamellar structure seemingly arising from eutectic transformation during high-speed heat treatment initiated by the pulsed electron beam (Fig. 4, *a*). X-ray spectral microanalysis of the foil indicates that the predominant element in layer *II* is aluminum (76.8 %), accompanied by smaller amounts of Mg (4.1 %), Cr (2.2 %), Mn (0.3 %), Fe (4.9 %), Co (1.6 %), Ni (10.1 %) (at. %).

Darkfield analysis, coupled with subsequent micro-electronogram identification, revealed that this layer is composed of plates corresponding to the follo-

Table 2

#### Results of micro-X-ray spectral analysis of the elemental composition of the surfacing – substrate system irradiated with a pulsed electron beam

Таблица 2. Результаты микрорентгеноспектрального анализа элементного состава системы «наплавка – подложка», облученной импульсным электронным пучком

Spectrum	Content, %							
	Mg	Al	Si	Cr	Mn	Fe	Co	Ni
Region A								
1	3.55	96.45	0	0	0	0	0	0
2	5.69	83.06	3.95	0.27	0.38	1.44	0.41	4.79
Region B								
1	3.00	97.00	0	0	0	0	0	0
2	10.73	80.65	2.43	0.29	0.31	1.25	0.33	4.02

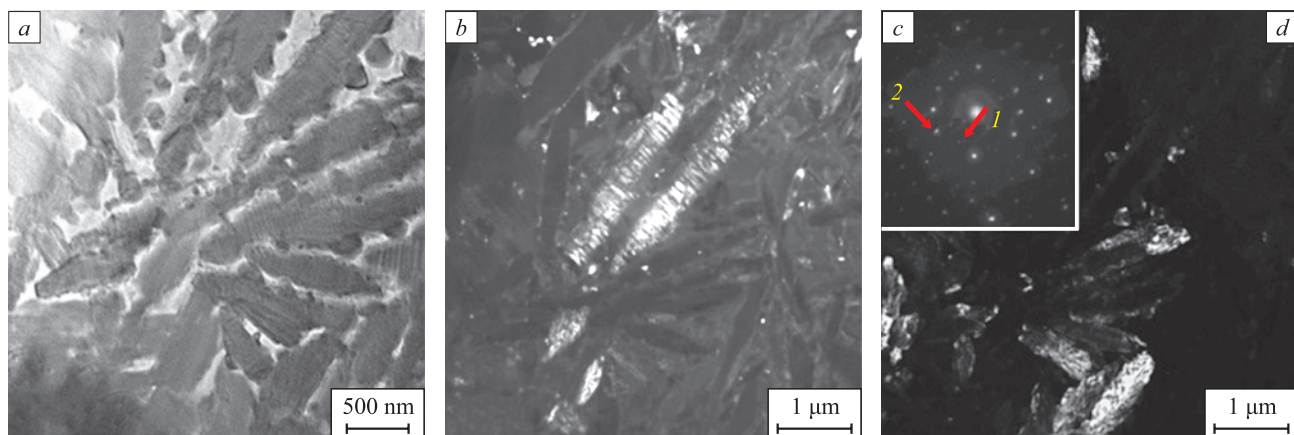


Fig. 4. Structure of layer II of the surfacing – substrate system:  
 а – светлопольное изображение; б, д – темнопольные изображения; в – микроэлектронограмма с участка фольги (а).  
 Изображение (б) получено в рефлексе  $[113]\text{Al}_{13}\text{Fe}_4$ ; изображение (д) получено в рефлексах  $[101]\text{Cr-Ni-Fe} + [114]\text{Al}_6\text{Fe}$ ;  
 на в (с) обозначены рефлексы, в которых получены темные поля 1 (б) и 2 (д)

Рис. 4. Структура слоя II системы «наплавка – подложка»:

а – светлопольное изображение; б, д – темнопольные изображения; в – микроэлектронограмма с участка фольги (а).  
 Изображение (б) получено в рефлексе  $[113]\text{Al}_{13}\text{Fe}_4$ ; изображение (д) получено в рефлексах  $[101]\text{Cr-Ni-Fe} + [114]\text{Al}_6\text{Fe}$ ;  
 на в (с) обозначены рефлексы, в которых получены темные поля 1 (б) и 2 (д)

wing phases:  $\text{Al}_{13}\text{Fe}_4$  (Fig. 4, b), Cr–Ni–Fe and  $\text{Al}_6\text{Fe}$  (Fig. 4, d).

Layer III, akin to layer I, consists of cells displaying high-speed crystallization (Fig. 5, a). The majority of these cells constitute an alloy with the composition 0.17 % Mg – 20.3 % Al – 4.3 % Cr – 16.7 % Fe – 9.3 % Co – 49.2 % Ni, aligning with a HEA doped with substrate elements. Interlayers of the second phase, situated along the boundaries of the cells, are also formed by elements from the surfacing and substrate (41.5 % Mg – 10.9 % Al – 9.0 % Cr – 1.0 % Mn – 15.2 % Fe – 4.1 % Co – 18.4 % Ni).

Darkfield analysis, along with microelectronogram indication, revealed that the bulk of high-speed crystallization cells in layer III is constituted by a solid solution based on HEA, doped with aluminum and magnesium (Fig. 5, b). These crystallization cells are separated by interlayers of the  $\text{Al}_{18}\text{Cr}_2\text{Mg}_3$  phase (Fig. 5, c).

## CONCLUSIONS

The wire-arc additive manufacturing method was employed to create a HEA coating with a non-equi-

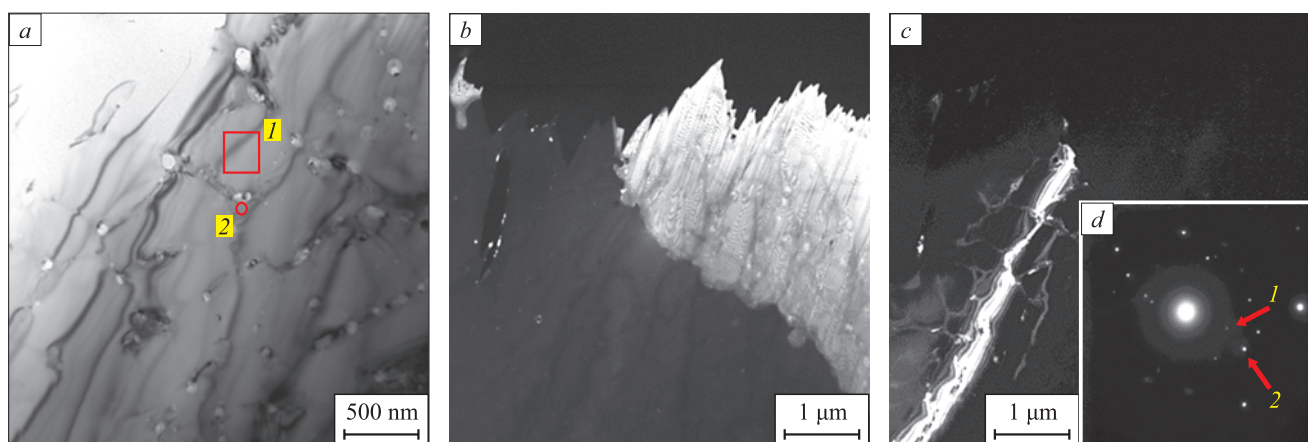


Fig. 5. Structure of layer III of the surfacing – substrate system after electron beam processing:  
 а – светлопольное изображение; б, в – темнопольные изображения и микроэлектронограмма (д), полученные с участка фольги (а).  
 Изображение (б) получено в рефлексе  $[210]\text{Cr-Ni-Fe}$ ; изображение (в) получено в рефлексах  $[222]\text{Cr-Ni-Fe} + [880]\text{Al}_{18}\text{Cr}_2\text{Mg}_3$ ;  
 на в (д) обозначены рефлексы, в которых получены темные поля 1 (б) и 2 (в)

Рис. 5. Структура слоя III системы «наплавка – подложка» после электронно-пучковой обработки:

а – светлопольное изображение; б, в – темнопольные изображения и микроэлектронограмма (д), полученные с участка фольги (а).  
 Изображение (б) получено в рефлексе  $[210]\text{Cr-Ni-Fe}$ ; изображение (в) получено в рефлексах  $[222]\text{Cr-Ni-Fe} + [880]\text{Al}_{18}\text{Cr}_2\text{Mg}_3$ ;  
 на в (д) обозначены рефлексы, в которых получены темные поля 1 (б) и 2 (в)

atomic elemental composition Mn–Cr–Fe–Co–Ni on alloy 5083. The contact zone of the coating – substrate system underwent irradiation with an intense pulsed electron beam. Through advanced techniques in physical materials science, investigations into the elemental and phase compositions, as well as the state of the defective substructure of the alloy formed in the contact zone of the substrate – coating system, were conducted. The analysis revealed mutual doping of the coating and substrate in a layer with an approximate thickness of 1700 µm. The high-speed cooling of the contact zone in the coating – substrate system, occurring under the thermal influence initiated by a pulsed electron beam, resulted in the formation of a multi-element, multi-phase submicro-nanocrystalline structure. The contact layer adjacent to the substrate exhibited a high-speed cellular crystallization structure, with the cell bulk formed by a solid solution of magnesium in aluminum, corresponding to alloy 5083. Interlayers of the second phase, enriched in atoms from both the coating and substrate, were observed along the cell boundaries. In the central region of the contact zone, plate-shaped crystallites were found, suggesting a potential eutectic nature of formation. The primary chemical element in this area was aluminum, constituting approximately 77 at. %. The contact layer adjacent to the coating displayed a high-speed cellular crystallization structure, with the majority of cells formed by an alloy composition (0.17 % Mg – 20.3 % Al – 4.3 % Cr – 16.7 % Fe – 9.3 % Co – 49.2 % Ni) corresponding to HEA, doped with substrate elements. Interlayers of the second phase, located along the boundaries of the cells, were enriched with magnesium and, to a lesser extent, with atoms forming the coating.

## REFERENCES / СПИСОК ЛИТЕРАТУРЫ

- Gromov V.E., Konovalov S.V., Ivanov Yu.F., Osintsev K.A. *Structure and Properties of High-Entropy Alloys*. Springer: Advanced Structured Materials; 2021;107:110. <https://doi.org/10.1007/978-3-030-78364-8>
- Osintsev K.A., Gromov V.E., Konovalov S.V., Ivanov Yu.F., Panchenko I.A. High-entropy alloys: Structure, mechanical properties, deformation mechanisms and application. *Izvestiya. Ferrous Metallurgy*. 2021;64(4):249–258. (In Russ.). <https://doi.org/10.17073/0368-0797-2021-4-249-258>
- Osinцев К.А., Громов В.Е., Коновалов С.В., Иванов Ю.Ф., Панченко И.А. Высокоэнтропийные сплавы: структура, механические свойства, механизмы деформации и применение. *Известия вузов. Черная металлургия*. 2021;64(4):249–258. <https://doi.org/10.17073/0368-0797-2021-4-249-258>
- Yeh J.-W., Chen S.-K., Lin S.-J., Gan J.-Y., Chin T.-S., Shun T.-T., Tsau C.-H., Chang S.-Y. Nanostructured high entropy alloys with multiple principal elements: Novel alloy design concepts and outcomes. *Advanced Engineering Materials*. 2004;6(5):299–303. <https://doi.org/10.1002/adem.200300567>
- Cantor B., Chang I.T.H., Knight P., Vincent A.J.B. Microstructural development in equiatomic multicomponent alloys. *Materials Science and Engineering: A*. 2004;375-377: 213–218. <https://doi.org/10.1016/j.msea.2003.10.257>
- Yeh J.-W., Chen Y.-L., Lin S.-J., Chen S.-K. High-entropy alloys – A new era of exploitation. *Materials Science Forum*. 2007;560:1–9. <https://doi.org/10.4028/www.scientific.net/MSF.560.1>
- Zhang Y., Yang X., Liaw P.K. Alloy design and properties optimization of high-entropy alloys. *JOM*. 2012;64(7): 830–838. <https://doi.org/10.1007/s11837-012-0366-5>
- Yeh J.-W. Recent Progress in high-entropy alloys. *European Journal of Control*. 2006;31(6):633–648. <https://doi.org/10.3166/acsm.31.633-648>
- Yeh J.-W. Alloy design strategies and future trends in high-entropy alloys. *JOM*. 2013;65(12):1759–1771. <https://doi.org/10.1007/s11837-013-0761-6>
- Zhang L.-S., Ma G.-L., Fu L.-C., Tian J.-Y. Recent progress in high-entropy alloys. *Advanced Materials Research*. 2013;631-632:227–232. <https://doi.org/10.4028/www.scientific.net/AMR.631-632.227>
- Zhang Y., Zuo T.T., Tang Z., Gao M.C., Dahmen K.A., Liaw P.K., Lu Z.P. Microstructures and properties of high-entropy alloys. *Progress in Materials Science*. 2014;61:1–93. <https://doi.org/10.1016/j.pmatsci.2013.10.001>
- Gali A., George E.P. Tensile properties of high- and medium-entropy alloys. *Intermetallics*. 2013;39:74–78. <https://doi.org/10.1016/j.intermet.2013.03.018>
- Li D.Y., Zhang Y. The ultrahigh charpy impact toughness of forged AlCoCrFeNi high entropy alloys at room and cryogenic temperatures. *Intermetallics*. 2016;70:24–28. <https://doi.org/10.1016/j.intermet.2015.11.002>
- Cantor B. Multicomponent and high entropy alloys. *Entropy*. 2014;16(9):4749–4768. <https://doi.org/10.3390/e16094749>
- Miracle D.B., Senkov O.N. A critical review of high entropy alloys and related concepts. *Acta Materialia*. 2017;122: 448–511. <https://doi.org/10.1016/j.actamat.2016.08.081>
- Zhang W., Liaw P.K., Zhang Y. Science and technology in high-entropy alloys. *Science China Materials*. 2018;61(1): 2–22. <https://doi.org/10.1007/s40843-017-9195-8>
- Tsai M.-H., Yeh J.-W. High-entropy alloys: a critical review. *Materials Research Letters*. 2014;2(3):107–123. <https://doi.org/10.1080/21663831.2014.912690>
- Alaneme K.K., Bodunrin M.O., Oke S.R. Processing, alloy composition and phase transition effect on the mechanical and corrosion properties of high entropy alloys: a review. *Journal of Materials Research and Technology*. 2016;5(4):384–393. <https://doi.org/10.1016/j.jmrt.2016.03.004>
- Osintsev K.A., Gromov V.E., Ivanov Yu.F., Konovalov S.V., Panchenko I.A., Vorobyov S.V. Evolution of structure in AlCoCrFeNi high-entropy alloy irradiated by pulsed electron beam. *Metals*. 2021;11(8):1228. <https://doi.org/10.3390/met11081228>
- Egerton F.R. *Physical Principles of Electron Microscopy*. Basel; 2016:96.
- Kumar C.S.S.R. *Transmission Electron Microscopy. Characterization of Nanomaterials*. New York; 2014:717.
- Carter C.B., Williams D.B. *Transmission Electron Microscopy*. Berlin; 2016:518.

## Information about the Authors

## Сведения об авторах

**Mikhail O. Efimov**, Postgraduate of the Chair of Science named after V.M. Finkel', Siberian State Industrial University

**ORCID:** 0000-0002-4890-3730

**E-mail:** moefimov@mail.ru

**Yuriy F. Ivanov**, Dr. Sci. (Phys.-Math.), Prof., Chief Researcher, Institute of High-Current Electronics, Siberian Branch of the Russian Academy of Sciences

**ORCID:** 0000-0001-8022-7958

**E-mail:** yufi55@mail.ru

**Viktor E. Gromov**, Dr. Sci. (Phys.-Math.), Prof., Head of the Chair of Science named after V.M. Finkel', Siberian State Industrial University

**ORCID:** 0000-0002-5147-5343

**E-mail:** gromov@physics.sibsiu.ru

**Yuliya A. Shlyarova**, Postgraduate of the Chair of Science named after V.M. Finkel', Researcher of Laboratory of Electron Microscopy and Image Processing, Siberian State Industrial University

**ORCID:** 0000-0001-5677-1427

**E-mail:** rubannikova96@mail.ru

**Irina A. Panchenko**, Cand. Sci. (Eng.), Head of the Laboratory of Electron Microscopy and Image Processing, Siberian State Industrial University

**ORCID:** 0000-0002-1631-9644

**E-mail:** i.r.i.ss@yandex.ru

**Михаил Олегович Ефимов**, аспирант кафедры естественнонаучных дисциплин им. профессора В.М. Финкеля, Сибирский государственный индустриальный университет

**ORCID:** 0000-0002-4890-3730

**E-mail:** moefimov@mail.ru

**Юрий Федорович Иванов**, д.ф.-м.н., профессор, главный научный сотрудник, Институт сильноточной электроники Сибирского отделения РАН

**ORCID:** 0000-0001-8022-7958

**E-mail:** yufi55@mail.ru

**Виктор Евгеньевич Громов**, д.ф.-м.н., профессор, заведующий кафедрой естественнонаучных дисциплин им. профессора В.М. Финкеля, Сибирский государственный индустриальный университет

**ORCID:** 0000-0002-5147-5343

**E-mail:** gromov@physics.sibsiu.ru

**Юлия Андреевна Шлярова**, аспирант кафедры естественнонаучных дисциплин им. профессора В.М. Финкеля, научный сотрудник лаборатории электронной микроскопии и обработки изображений, Сибирский государственный индустриальный университет

**ORCID:** 0000-0001-5677-1427

**E-mail:** rubannikova96@mail.ru

**Ирина Алексеевна Панченко**, к.т.н., заведующий лабораторией электронной микроскопии и обработки изображений, Сибирский государственный индустриальный университет

**ORCID:** 0000-0002-1631-9644

**E-mail:** i.r.i.ss@yandex.ru

## Contribution of the Authors

## Вклад авторов

**M. O. Efimov** – coating of Mn – Cr – Fe – Co – Ni HEA on the substrate of alloy 5083, writing the text.

**Yu. F. Ivanov** – conducting electron microscopic studies, analysis of the results.

**V. E. Gromov** – formation of the research concept, analysis of TEM images, writing the text.

**Yu. A. Shlyarova** – literary review, preparation of the HEA constituent elements, design of the article.

**I. A. Panchenko** – irradiation of the samples, analysis of the results, writing the text.

**М. О. Ефимов** – нанесение покрытия ВЭС состава Mn – Cr – Fe – Co – Ni на подложку сплава 5083, написание статьи.

**Ю. Ф. Иванов** – проведение электронно-микроскопических исследований, анализ результатов.

**В. Е. Громов** – формирование концепции работы, анализ ПЭМ изображений, написание статьи.

**Ю. А. Шлярова** – обзор литературы, подготовка составляющих элементов ВЭС, оформление статьи.

**И. А. Панченко** – облучение образцов, анализ результатов, написание статьи.

Received 02.06.2023

Revised 15.07.2023

Accepted 11.09.2023

Поступила в редакцию 02.06.2023

После доработки 15.07.2023

Принята к публикации 11.09.2023